



Universiteit  
Leiden  
The Netherlands

## **Cysteine ligand vibrations are responsible for the complex resonance Raman spectrum of azurin**

Andrew, C.R.; Han, J.; Blaauwen, T. den; Pouderoyen, G. van; Vijgenboom, E.; Canters, G.W.; ... ; Sanders-Loehr, J.

### **Citation**

Andrew, C. R., Han, J., Blaauwen, T. den, Pouderoyen, G. van, Vijgenboom, E., Canters, G. W., ... Sanders-Loehr, J. (1997). Cysteine ligand vibrations are responsible for the complex resonance Raman spectrum of azurin. *Journal Of Biological Inorganic Chemistry*, 2(1), 98-107. doi:10.1007/s007750050111

Version: Publisher's Version

License: [Licensed under Article 25fa Copyright Act/Law \(Amendment Taverne\)](#)

Downloaded from: <https://hdl.handle.net/1887/3239412>

**Note:** To cite this publication please use the final published version (if applicable).

## ORIGINAL ARTICLE

Colin R. Andrew · Jane Han · Tanneke den Blaauwen  
Gertie van Pouderoyen · Erik Vijgenboom  
Gerard W. Canters · Thomas M. Loehr  
Joann Sanders-Loehr

## Cysteine ligand vibrations are responsible for the complex resonance Raman spectrum of azurin

Received: 29 July 1996 / Accepted: 9 November 1996

**Abstract** In the redox center of azurin, the Cu(II) is strongly coordinated to one thiolate S from Cys 112 and two imidazole Ns from His 46 and 117. This site yields a complex resonance Raman (RR) spectrum with >20 vibrational modes between 200 and 1500  $\text{cm}^{-1}$ . We have investigated the effects of *ligand-selective* isotope replacements on the RR spectrum of *Pseudomonas aeruginosa* azurin to determine the relative spectral contribution from each of the copper ligands. Growth on  $^{34}\text{S}$ -sulfate labels the cysteine ligand and allows the identification of a cluster of bands with Cu–S(Cys) stretching character between 370 and 430  $\text{cm}^{-1}$  whose frequencies are consistent with the trigonal or distorted tetrahedral coordination in type 1 sites. In type 2 copper-cysteinate sites, the lower  $\nu(\text{Cu–S})$  frequencies between 260 and 320  $\text{cm}^{-1}$  are consistent with square-planar coordination. Addition of *exogenous*  $^{15}\text{N}$ -labeled imidazole or histidine to the His117Gly mutant generates type 1 or type 2 sites, respectively. Because neither the above nor the His46Gly mutant reconstituted with  $^{15}\text{N}$ -imidazole exhibits significant isotope dependence, the histidine ligands can be ruled out as important contributors to the RR spectrum. Instead, a variety of evidence, including extensive isotope shifts upon global substitution with  $^{15}\text{N}$ , suggests that the multiple RR modes of azurin are due principally to vibrations of the cysteine ligand. These are resonance-enhanced through kinematic coupling with the Cu–S stretch in the ground state or through an excited-state A-term mechanism involving a Cu-cysteinate chromophore that extends into the peptide backbone.

**Key words** Azurin · Cupredoxin · Copper-cysteinate protein · Resonance Raman spectroscopy · Vibrational assignments

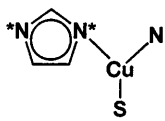
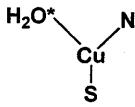
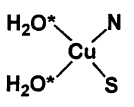
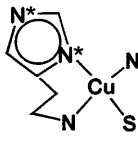
### Introduction

Cupredoxins are a class of evolutionarily related electron transfer proteins containing a copper-cysteinate redox center embedded in an eight-stranded  $\beta$  barrel. The most well-known examples are the mononuclear Cu-Cys centers of blue Cu proteins such as azurin and plastocyanin [1, 2]. The X-ray crystal structures of these proteins in their Cu(II) states reveal a conserved set of strongly bound ligands consisting of a cysteine S and two histidine imidazole Ns in a trigonal array [2]. A weak fourth ligand (usually methionine S) lies above the trigonal plane in an axial position, and, in the case of azurin, another weak interaction is present from the peptide carbonyl O of glycine [3, 4]. These trigonal sites are classified as *type 1* on the basis of their small EPR Cu(II) hyperfine splitting ( $<90 \times 10^{-4} \text{cm}^{-1}$ ) and intense charge transfer (CT) absorption maximum near 600 nm (Fig. 1). Addition of a fourth strong ligand by mutagenesis can result in a tetragonal *type 2* geometry, having a substantially larger  $A_{\parallel}$  of  $>140 \times 10^{-4} \text{cm}^{-1}$  and higher energy absorption maximum near 400 nm [5].

Resonance Raman (RR) spectroscopy, a vibrational technique that selectively probes charge transfer chromophores, provides a more quantitative description of copper-cysteinate structures [6, 7]. Excitation within the (Cys)S $\rightarrow$ Cu(II) CT band leads to the enhancement of five or more fundamental vibrations between 250 and 500  $\text{cm}^{-1}$ . Studies of an extensive series of copper-cysteinate proteins have shown that a *single, predominant* Cu–S stretching mode can be identified by its large frequency shift upon S- (or Cu-) isotope substitution, its high intensity, and its singular ability to generate combination bands [7, 8]. The frequency of the Cu–S(Cys) stretching vibration,  $\nu(\text{Cu–S})$ , acts as a sensitive

C.R. Andrew · J. Han · T.M. Loehr · J. Sanders-Loehr (✉)  
Department of Chemistry, Biochemistry and Molecular Biology,  
Oregon Graduate Institute of Science & Technology,  
Portland, OR 97291-1000, USA  
Tel.: +1-503-690-1079; Fax: +1-503-690-1464;  
e-mail: joann@admin.ogi.edu

T. den Blaauwen · G. van Pouderoyen · E. Vijgenboom  
G.W. Canters  
Leiden Institute of Chemistry, Gorlaeus Laboratories,  
2300 RA Leiden, The Netherlands

	Type 1		Type 2	
				
	H117G(Im-1)	H117G(Aqua-1)	H117G(Aqua-2)	H117G(His-2)
$\lambda_{\max}$	625	628	420	400
$\nu(\text{Cu-S})$	406	397	298	319

**Fig. 1** Proposed coordination geometries for adducts of azurin-H117G with exogenous imidazole (Im), water (Aqua) or histidine (His) ligands. Type 1 copper sites are indicated by Im-1 or Aqua-1, whereas type 2 sites are indicated by Aqua-2 or His-2. This copper site classification is based on absorption maxima ( $\lambda_{\max}$  in nm) and Raman stretching frequencies [ $\nu(\text{Cu-S})$  in  $\text{cm}^{-1}$ ], as well as EPR properties [11, 12]. The locations of isotopically labeled atoms of exogenous ligands are indicated by (\*)

indicator of the Cu-S bond length to a degree of accuracy that is probably beyond the  $\pm 0.05 \text{ \AA}$  limits of X-ray crystallography [7, 9]. The  $\nu(\text{Cu-S})$  frequency (Fig. 1) also provides a measure of the coordination geometry, with values ranging from 405–430  $\text{cm}^{-1}$  for trigonal planar to 340–360  $\text{cm}^{-1}$  for tetrahedral and 300–320  $\text{cm}^{-1}$  for tetragonal Cu sites [7]. The Cu-S stretch is the only metal-ligand vibrational mode that has been definitively assigned in the RR spectra of cupredoxins.

The prime focus of the present investigation was to determine the relative contributions of the cysteine and histidine ligands to the RR spectrum of azurin by selectively incorporating heavy isotopes into the different ligands. Thus, global replacement of S or N was accomplished by growth on  $^{34}\text{S}$ -sulfate or  $^{15}\text{N}$ -ammonia. In addition, the availability of His(ligand)→Gly mutants with exogenous ligand-binding ability [5] has made it possible to substitute either His46 or His117 with  $^{15}\text{N}$ -imidazole [10, 11]. The loss of a covalent link to the peptide backbone in the His→Gly mutants also increases the flexibility of the Cu site, thereby allowing a variety of coordination geometries to be achieved by the addition of different exogenous ligands to the cavity [10, 11]. Thus, addition of monodentate ligands such as imidazole or water to the His(ligand)→Gly mutants restores the trigonal type 1 coordination of wild-type azurin [12]. This is evidenced by an absorption maximum near 620 nm as well as a  $\nu(\text{Cu-S})$  near 400  $\text{cm}^{-1}$  that is indicative of a short Cu-S(Cys) bond (Fig. 1). In contrast, addition of a bidentate ligand such as histidine leads to the formation of a tetragonal type 2 complex with a  $\nu(\text{Cu-S})$  frequency of 319  $\text{cm}^{-1}$  [H117G(His-2) in Fig. 1]. The 86- $\text{cm}^{-1}$  downshift of the most intense RR peak is consistent with a weakening of the Cu-S(Cys) bond in response to the coordination of a fourth strong ligand in the equatorial plane [7]. In many cases, an equilibrium mixture of type 1 and type 2 species is

actually observed. For example, in H117G azurin at pH 6 with no added exogenous ligands, RR spectra reveal distinct Aqua-1 and Aqua-2 species (Fig. 1) that can be distinguished by excitation within their respective absorption bands at 628 and 420 nm [12]. The possibility of Cu-OH<sub>2</sub> modes in the RR spectra of these aqua complexes was probed using H<sub>2</sub><sup>16</sup>O and H<sub>2</sub><sup>18</sup>O.

We found that neither the coordinated imidazoles nor the coordinated water molecules made any significant contribution to the RR spectra. In contrast, extensive N-isotope shifts occurred for azurins that had been globally  $^{15}\text{N}$ -labeled during biosynthesis, suggesting the involvement of backbone amide vibrations, with the cysteine ligand being the most likely candidate. This is supported by the observation of a resonance-enhanced cysteine S-C stretch near 750  $\text{cm}^{-1}$  as well as a number of other high frequency cysteine fundamentals. Two factors appear to be responsible for the enhancement of cysteine ligand vibrations in the RR spectrum of azurin: (1) kinematic (ground state) coupling of the Cu-S stretch with vibrations of the coplanar Cu-S<sub>γ</sub>-C<sub>β</sub>-C<sub>α</sub>-N moiety [13] and (2) vibronic coupling of vibrational and electronic transitions of the entire copper-cysteinate moiety. The cysteine ligand is thus seen to be central to controlling the copper-site spectroscopy, coordination geometry, and function of cupredoxins.

## Materials and methods

Wild-type azurin from *Pseudomonas aeruginosa* was obtained by expression of a cloned *azu* gene in *Escherichia coli* as described previously [14]. The  $^{15}\text{N}$ -enriched azurin was obtained by growing the cells on  $^{15}\text{N}$ -ammonium chloride as their sole nitrogen source, resulting in the uniform N-labeling of all side chains as well as the main chain of the protein [14]. The azurin-H117G mutant from *Ps. aeruginosa* was expressed in *E. coli* and the imidazole, D-L histidine, and aqua adducts of H117G were prepared as previously described [12, 15] from ligands containing natural abundance atoms or their heavy isotope counterparts:  $^{15}\text{N}$ -imidazole (double-labeled, 99 atom %, Isotech),  $^{15}\text{N}$ -(D-L)-histidine (ring-only labeled, 99 atom %, ICON) and H<sub>2</sub><sup>18</sup>O (95 atom %, ICON). The  $^{34}\text{S}$ -enriched H117G-azurin was obtained by growing cells on  $^{34}\text{S}$ -sulfate (90 atom %, ICON) as described previously [7].

For Cu isotope substitution, metallic  $^{65}\text{Cu}$  (99.7 atom %) and  $^{63}\text{Cu}$  (99.2 atom %) were purchased from Intersales-Holland and converted to Cu(NO<sub>3</sub>)<sub>2</sub> by dissolving 10 mg of Cu in 50 ml of 70% HNO<sub>3</sub>. The Cu solutions were diluted to 5 ml and adjusted to pH 2, then added in a stoichiometric amount to 0.1 mM apo-

H117G in 20 mM MES (pH 5.0) to generate the yellow-green aqua species. After maximum Cu binding was achieved based on  $A_{420}$  (~30 min), a 30-fold excess of imidazole was added to generate the blue species. Raman samples of wild-type and H117G-azurin contained 2–4 mM protein in 20 mM MES (pH 6.0).

The azurin-H46G mutant from *Ps. aeruginosa* was expressed in *E. coli* and purified as previously described [10]. The  $^{14}\text{N}$ - and  $^{15}\text{N}$ -imidazole adducts of H46G used for RR measurements were prepared from solutions of apo H46G (17  $\mu\text{l}$ , 4.7 mM) in 0.06 M HEPES (pH 7.5) by the addition of 0.8  $\mu\text{l}$  0.1 M  $\text{Cu}(\text{NO}_3)_2$  and 2  $\mu\text{l}$  of 250 mM imidazole to give a sixfold ligand excess. For H46G(Aqua) samples, 30  $\mu\text{l}$  of 5 mM apoprotein was diluted tenfold with either  $\text{H}_2^{16}\text{O}$  or  $\text{H}_2^{18}\text{O}$  and reconcentrated to 30  $\mu\text{l}$  by ultrafiltration (Microcon device, Amicon), followed by addition of 1.6  $\mu\text{l}$  of 0.1 M  $\text{Cu}(\text{NO}_3)_2$  and 2  $\mu\text{l}$  of 1 M MES (pH 5.5). The final pH of the protein sample was checked using an MI-410 microelectrode (Microelectrodes) and adjusted if necessary with 1  $\mu\text{l}$  aliquots of 0.1 M NaOH or  $\text{HNO}_3$ . Care was taken to avoid  $\text{Cl}^-$  contamination of either the protein or buffer solutions from the pH electrode by making pH measurements on separate aliquots. Raman samples of H46G-azurin contained 4 mM protein in 0.05 M HEPES (pH 7.5) for imidazole adducts or in 0.06 M MES (pH 5.5) for aqua adducts.

Most of the Raman spectra were recorded on a modified Jarrell-Ash 25-300 spectrophotometer equipped with an Ortec Model 9302 amplifier/discriminator and a cooled ( $-30^\circ\text{C}$ ) RCA C31034 photomultiplier that was interfaced to an Intel 310 computer. Alternatively (as specifically noted below) Raman spectra were collected using a custom McPherson 2061/207 spectrograph (0.67 m, 1800-groove grating) with a Princeton Instruments (LN-1100PB) liquid  $\text{N}_2$ -cooled CCD detector; Rayleigh scattering was attenuated with either a Kaiser Optical holographic super-notch filter or a McPherson 270 double monochromator (600-groove grating) pre-filter stage. All spectra were collected in an  $\sim 150^\circ$  backscattering geometry from samples maintained at 15 K by use of a closed-cycle helium refrigerator (Air Products, Displex) [16]. The desired excitation wavelengths were provided by the following lasers: Spectra-Physics 2025-11 Kr, Spectra-Physics 164 Ar, Licorix He-Cd 4240 NB, Coherent Innova 90-6 Ar, and Coherent 599-01 Dye (rhodamine 6G). Absolute frequencies, obtained by calibration with  $\text{CCl}_4$  or indene, are accurate to  $\pm 1 \text{ cm}^{-1}$ . Isotope shifts, obtained from spectra recorded under identical experimental conditions, have been evaluated by abscissa expansion and curve resolution of overlapping bands and are accurate to  $\pm 0.5 \text{ cm}^{-1}$ . Although all of the spectra reported in the present work were obtained at 15 K, spectra taken at ice temperature revealed similar peak frequencies and isotope shifts, albeit with poorer spectral resolution. We did not observe the temperature-dependent changes in frequencies and intensities that had been suggested in an earlier RR study of azurins [22].

## Results

### Cysteine S labeling and the Cu–S stretch

The RR spectrum of the imidazole adduct of azurin-H117G, obtained by excitation within its intense 625-nm (Cys)S $\rightarrow$ Cu(II) CT band, exhibits 12 bands in the Cu-ligand stretching region between 250 and 500  $\text{cm}^{-1}$  (Fig. 2A, Table 1), whose frequencies and intensities are similar to those observed for wild-type azurin (Fig. 2C). This indicates that the Cu binds exogenous imidazole in the H117G mutant in the same manner that it coordinates the imidazole ring of His117, thereby generating the same type 1 site (Fig. 1). Growth of bacteria on  $^{34}\text{S}$ -sulfate results in the global labeling of all Cys and Met residues in azurin. In the resultant RR

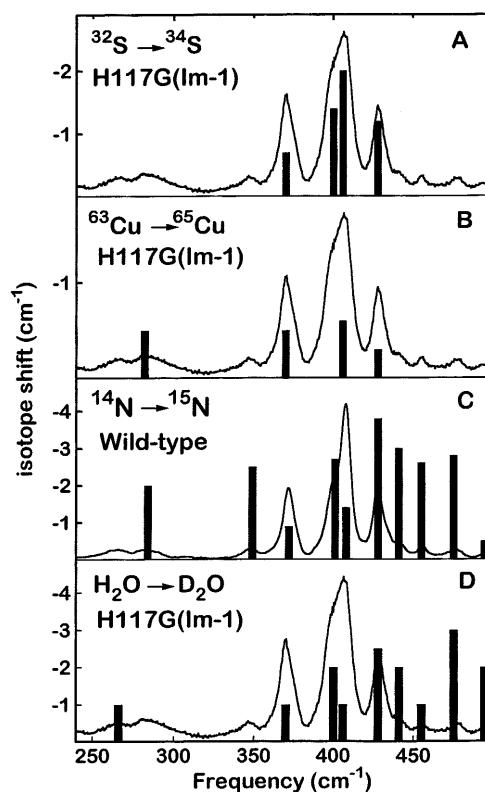


**Fig. 2A–D** Effect of global isotope exchange on the resonance Raman spectra of type 1 sites. Extent of frequency downshift in  $^{34}\text{S}$ ,  $^{65}\text{Cu}$ ,  $^{15}\text{N}$ , or  $\text{D}_2\text{O}$  shown as bars and quantitated on the y axis. **A** Imidazole adduct of H117G-azurin prepared from cells grown on  $^{32}\text{S}$ - or  $^{34}\text{S}$ -sulfate. **B** Imidazole adduct of H117G-azurin reconstituted with  $^{63}\text{Cu}(\text{NO}_3)_2$  or  $^{65}\text{Cu}(\text{NO}_3)_2$ . **C** Wild-type azurin prepared from cells grown on  $^{14}\text{N}$ - or  $^{15}\text{N}$ -ammonia. **D** Imidazole adduct of H117G-azurin equilibrated in either  $\text{H}_2\text{O}$  or  $\text{D}_2\text{O}$  prior to reconstitution with Cu. All RR spectra were obtained using 647-nm excitation (70–100 mW) at a scan rate of  $0.5 \text{ cm}^{-1}\text{s}^{-1}$ , spectral resolution of 4–5  $\text{cm}^{-1}$ , and accumulation of 4–10 scans

spectrum, the most intense feature at 406  $\text{cm}^{-1}$  undergoes the greatest  $^{34}\text{S}$  shift of  $-2.0 \text{ cm}^{-1}$  (Fig. 2A, Table 1), revealing that it has the most Cu–S stretching character. The high energy of this vibration is indicative of a short Cu–S(Cys) bond distance, similar to the 2.13-Å value observed in wild-type azurin [3, 17]. However, there is actually a cluster of  $\nu(\text{Cu–S})$  modes rather than a single RR mode (Fig. 2A), owing to the coupling of the Cu–S stretch with other cysteine ligand vibrations. Thus, the flanking modes at 370, 401, and 428  $\text{cm}^{-1}$  have  $^{34}\text{S}$  shifts of  $-0.7$ ,  $-1.4$  and  $-1.2 \text{ cm}^{-1}$ , respectively, which are similar to the  $^{34}\text{S}$  shifts in wild-type azurin (Table 1) [8].

Substitution of  $^{65}\text{Cu}$  for  $^{63}\text{Cu}$  in the H117G(Im-1) adduct confirms that the maximum  $\nu(\text{Cu–S})$  character is associated with the most intense band at 406  $\text{cm}^{-1}$  (shift of  $-0.6 \text{ cm}^{-1}$ ), with additional vibrational coupling occurring at 372 ( $-0.5$ ) and 428 ( $-0.3$ )  $\text{cm}^{-1}$  (Fig. 2B, Table 1). A general correlation is observed between the extent of the S and Cu isotope shifts and the peak intensities. Thus, it appears that the most intense peaks in

**Table 1** Raman frequencies for type 1 sites in azurins

Azurin	Raman frequency and isotope shifts to lower energy (cm <sup>-1</sup> )											
Wild-type	267	284	286	348	372	400	408	428	442	456	476	494
<sup>32</sup> S→ <sup>34</sup> S <sup>a</sup>					-0.4		-3.8	-1.4				
<sup>63</sup> Cu→ <sup>65</sup> Cu <sup>b</sup>					-0.6	-0.6	-0.6	-0.2				
<sup>14</sup> N→ <sup>15</sup> N (all)		-2	-1	-2.5	-0.9	-2.7	-1.4	-3.8	-3	-2.6	-2.8	-0.5
H <sub>2</sub> O→D <sub>2</sub> O		-2			-1	-2	-1	-1.5	-1.8	-0.7	-1.5	
H117G (Im-1)	266	282	286	348	370	401	406	428	442	455	473	494
<sup>32</sup> S→ <sup>34</sup> S					-0.7	-1.4	-2.0	-1.2				
<sup>63</sup> Cu→ <sup>65</sup> Cu			-1		-0.5		-0.6	-0.3				
<sup>14</sup> N→ <sup>15</sup> N-Im			-1									
H <sub>2</sub> O→D <sub>2</sub> O	-1				-1	-2	-1	-2.5	-2	-1	-3	-2
H117G (Aqua-1) <sup>c</sup>	261	302		346	368	397	406	428	440	455	477	493
H <sub>2</sub> O→D <sub>2</sub> O		-1				-1		-3			-3	
H46G (Im-1) <sup>d</sup>	263			346	369	397	408	427	439	455	475	492

<sup>a</sup> Data from [8]<sup>c</sup> No isotope shifts detected with H<sub>2</sub><sup>18</sup>O<sup>b</sup> Data from [22]<sup>d</sup> No isotope shifts detected with <sup>15</sup>N-imidazole

the RR spectrum of azurin all have substantial Cu–S stretching contributions.

#### Imidazole N labeling and the Cu–N stretch

The specific RR contribution of the His46 and His117 ligands was probed by reconstitution of either the H46G or H117G mutant with <sup>15</sup>N-imidazole. Excitation

of the H46G(Im-1) adduct at 647.1 nm yields a type 1 RR spectrum (Fig. 3C) similar to that of wild-type (Fig. 3A) and the H117G(Im-1) adduct (Fig. 3B). Thus, the trigonal type 1 copper site geometry appears to be conserved in the H46G(Im-1) adduct, although the peak near 280 cm<sup>-1</sup> is absent. In the <sup>15</sup>N-imidazole complexes of either mutant, none of the nine well-resolved RR peaks shows any N-isotope dependence (Fig. 3B,C). A closer examination of the 200–300 cm<sup>-1</sup> region where a Cu–N(Im) stretch is expected (because the imidazole behaves as a point mass of 68) shows that the H117G(Im-1) complex does exhibit a small decrease in the intensity of the 286-cm<sup>-1</sup> shoulder (Fig. 4B), suggesting an <sup>15</sup>N-downshift of ~1 cm<sup>-1</sup>. The H117G(Im-1) complex prepared from azurin reconstituted with <sup>65</sup>Cu shows a similar drop in the intensity of the 286 cm<sup>-1</sup> shoulder (Fig. 4C). Thus, it is likely that there is a Cu–N(Im) stretching contribution from H117 to the 286-cm<sup>-1</sup> vibrational mode in wild-type azurin (Fig. 4A). The lack of any other imidazole-dependent isotope shifts for the H46G and H117G complexes with exogenous imidazole suggests that the histidine ligands make a very minor contribution to the RR spectrum of azurin and that coordinated imidazoles do not undergo significant kinematic or vibronic coupling with the Cu–S(Cys) chromophore.

#### Global N labeling and peptide NH vibrations

Wild-type azurin was uniformly labeled with <sup>15</sup>N by growing bacteria on <sup>15</sup>N-ammonium chloride as the sole nitrogen source [14]. This technique labels not only the nitrogen atoms in the His46 and His117 ligands to copper, but also all other N atoms in side-chains and the peptide amide backbone. In contrast to results with <sup>15</sup>N-imidazole, where no significant shifts were observed, global <sup>15</sup>N-labeling results in a profusion of N isotope downshifts (Fig. 3A). Furthermore, unlike the S and Cu isotope shifts, which were concentrated in the four strongest modes between 370 and 430 cm<sup>-1</sup>

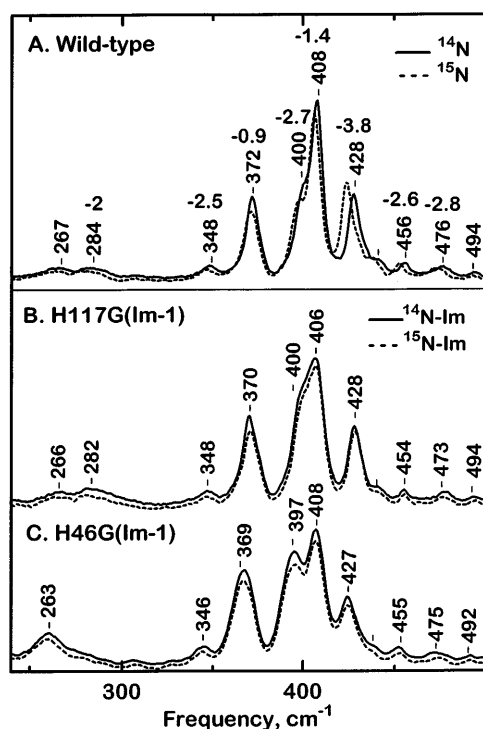


**Fig. 3A–C** Effect of <sup>15</sup>N (broken line) for <sup>14</sup>N (solid line) substitution on the Raman spectra of type 1 sites. **A** Wild-type azurin globally labeled by growing cells grown on <sup>14</sup>N- or <sup>15</sup>N-ammonia. **B** Imidazole adduct of H117G-azurin prepared by addition of exogenous <sup>14</sup>N- or <sup>15</sup>N-imidazole. **C** Imidazole adduct of H46G-azurin prepared by addition of exogenous <sup>14</sup>N- or <sup>15</sup>N-imidazole. All spectra obtained as in Fig. 2 except for **A** which used 160-mW excitation and 32 accumulations

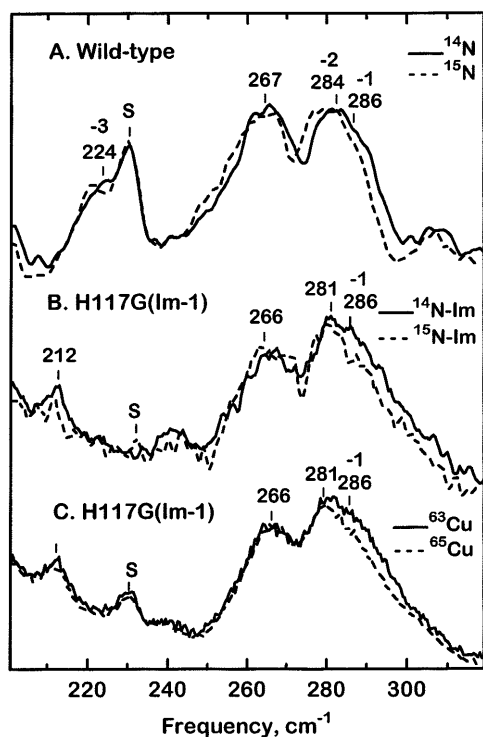


**Fig. 4A–C** Effect of N and Cu isotope substitution on the low-frequency RR spectra of type 1 sites. **A** Wild-type azurin globally labeled by growing cells on  $^{14}\text{N}$  (solid line) or  $^{15}\text{N}$  (broken line) from ammonia. **B** Imidazole adduct of H117G-azurin prepared by addition of exogenous  $^{14}\text{N}$  (solid line) or  $^{15}\text{N}$  (broken line) from imidazole. **C** Imidazole adduct of H117G azurin reconstituted with  $^{63}\text{Cu}$  (solid line) or  $^{65}\text{Cu}$  (broken line). Spectra **A** and **B** are expanded regions of Figs 3B and 3C, respectively. The spectra in **C** were obtained as in Fig. 2B, but with 25 accumulations

(Fig. 2A,B), the N dependence follows a totally different pattern, with 11 of the 12 RR bands undergoing shifts of 1 to 4  $\text{cm}^{-1}$  (Fig. 2C, Table 1). A similarly broad distribution of  $^{15}\text{N}$  shifts upon global N labeling has been observed in the RR spectrum of another type 1 protein, plastocyanin [18]. The total combined  $^{15}\text{N}$  shift of  $\sim 17 \text{ cm}^{-1}$  for wild-type azurin (Table 1) is far greater than that expected for a Cu–N(Im) stretch, which has a predicted  $^{15}\text{N}$  downshift of only  $\sim 2 \text{ cm}^{-1}$  [19]. This result clearly points to a significant vibrational contribution from nitrogen atoms beyond the first coordination sphere. The most obvious candidate is the amide nitrogen which connects the cysteine ligand to the polypeptide backbone. Previous studies have suggested that coupling of the amide nitrogen vibrations with those of the Cu–cysteinate moiety is facilitated by the coplanarity of the Cu–S $_{\gamma}$ –C $_{\beta}$ –C $_{\alpha}$ –N moiety [13]. However, the magnitude of the total  $^{15}\text{N}$  shift points to the involvement of additional N atoms and has led to the proposal that amide nitrogens of adjacent residues are also contributing to the vibrational spectrum [20].

Another potential measure of amide NH involvement comes from  $\text{D}_2\text{O}$  exchange. When the apoprotein from H117G azurin is equilibrated in  $\text{D}_2\text{O}$ , followed by

reconstitution with Cu and imidazole at pH 6.0, most of the RR bands downshift by 1 to 3  $\text{cm}^{-1}$  (Fig. 2D). Because this pattern of shifts is most reminiscent of the globally  $^{15}\text{N}$ -labeled protein (Fig. 2C), it suggests that the observed D dependence is due primarily to exchange of the peptide NH. An earlier proposal that the D shifts were due to the histidine imidazole ligands [19] can be ruled out by the fact that many more vibrational modes in the H117G(Im-1) adduct are affected by D substitution than by  $^{15}\text{N}$ -imidazole substitution (Fig. 3B). Similarly, the proposed H-bonding of the cysteine sulfur ligands [13, 21] is also unlikely because the D shifts differ significantly from  $^{34}\text{S}$  substitution (Fig. 3A), indicating that they are not correlated with  $\nu(\text{Cu–S})$  character. Deuterium shifts similar to those for H117G(Im-1) are observed for (1) wild-type azurin incubated in  $\text{D}_2\text{O}$  for 24 h at pH 6.0 [22], (2) wild-type azurin incubated for 1 d at 20°C, followed by a further 2 d at 4°C at pH 8.5 to promote base-catalyzed exchange (Table 1), and (3) the H117G(Aqua-1) complex (Fig. 1) with no exogenous imidazole (Table 1). From these findings, we can conclude that neither the imidazole side-chain nor the amide of His117 is a significant contributor to the D dependence. Rather, the combined data point to the peptide NH of the Cys 112 ligand as a major source. However, NMR studies of wild-type azurin, prepared under conditions similar to (2) above, gave no evidence for D exchange in the amide NH groups of residues 110 through 113 [14]. Nevertheless, we found that equilibration of apo-H117G azurin with  $\text{D}_2\text{O}$  for 24 h prior to reconstitution with Cu and imidazole yielded the same extent of D exchange as in the wild-type protein (Table 1), suggesting that the amide NH groups were relatively accessible to solvent in both cases.

#### Cu–N and Cu–O vibrations of type 2 sites

Reconstitution of H117G-azurin with histidine results in a type 2 species (His-2 in Fig. 1), proposed to arise from the bidentate chelation of the imidazole and  $\alpha$ -amino groups of the exogenous histidine. The RR spectrum of the H117G(His-2) complex exhibits its greatest intensity and S isotope dependence in the features at 259, 296, and 319  $\text{cm}^{-1}$  (Fig. 5A, Table 2). The fact that the Cu–S vibrational frequencies have decreased by  $\sim 100 \text{ cm}^{-1}$  compared to type 1 copper sites is commensurate with a  $\sim 0.15\text{-\AA}$  lengthening of the Cu–S(Cys) bond due to the addition of a fourth strong ligand and formation of a square-planar array [12]. Reconstitution of H117G(His-2) with  $^{15}\text{N}$ -ring-labeled histidine yields only a  $-0.9 \text{ cm}^{-1}$  shift in the 259  $\text{cm}^{-1}$  peak (Fig. 5A), implying that neither Cu–N or internal vibrations of the imidazole ring contribute significantly to the type 2 RR spectrum. This conclusion is supported by the similarity of the RR spectrum of H117G(His-2) with that of the H117G(Aqua-2) species (Fig. 6B), which is missing one of its original imidazole ligands. Reconstitution of the

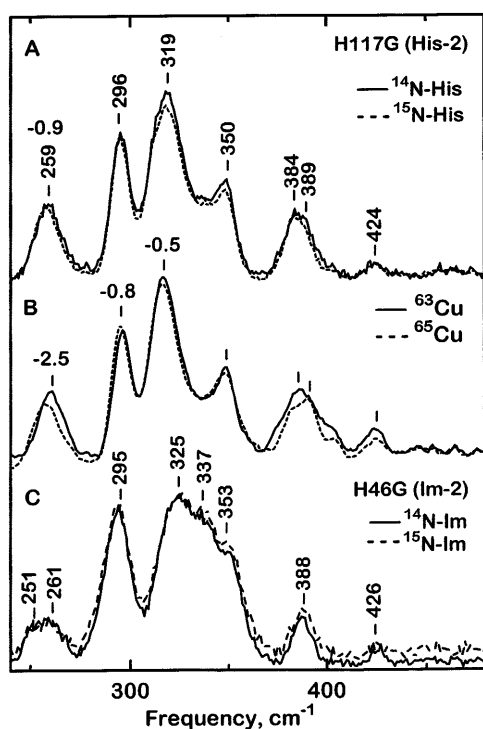


**Fig. 5A–C** Effect of N and Cu isotope substitution on the RR spectra of type 2 sites. **A** Histidine adduct of H117G-azurin (8 mM) prepared by the addition of  $^{14}\text{N}$  (solid line) or  $^{15}\text{N}$  (broken line) from histidine. **B** Histidine adduct of H117G-azurin reconstituted with  $^{63}\text{Cu}$  (solid line) or  $^{65}\text{Cu}$  (broken line). **C** Imidazole adduct of H46G-azurin prepared by the addition of  $^{14}\text{N}$  (solid line) or  $^{15}\text{N}$  (broken line) from imidazole. All RR spectra obtained with 407- or 413-nm excitation (25–40 mW) at a scan rate of  $0.5\text{ cm}^{-1}\text{ s}^{-1}$ , a spectral resolution of  $5\text{--}7\text{ cm}^{-1}$ , and 8–10 accumulations

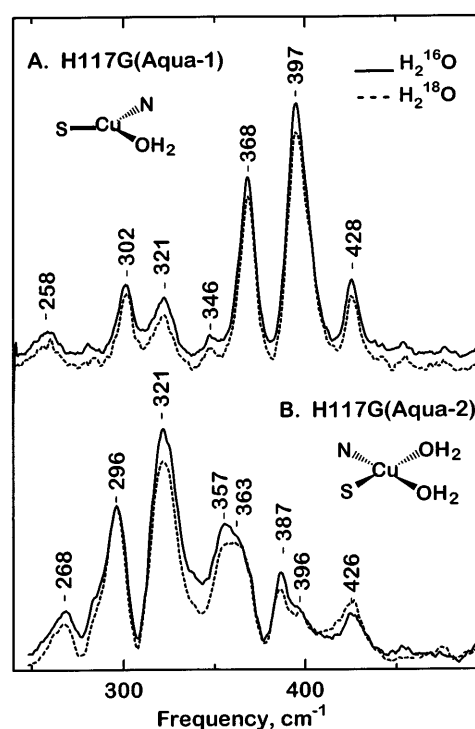


**Fig. 6A,B** Effect of  $\text{H}_2^{18}\text{O}$  (broken line) for  $\text{H}_2^{16}\text{O}$  (solid line) substitution on the Raman spectra of type 1 and type 2 aqua adducts. **A** Aqua-1 form H117G-azurin (pH 6.0) with no added ligands. Spectra obtained with 647-nm excitation as in Fig. 2. **B** Aqua-2 form of H117G-azurin (pH 6.0) with no added ligands. Spectra obtained on a McPherson spectrograph using 442-nm excitation (20 mW), 2400-groove grating, a spectral resolution of  $5\text{ cm}^{-1}$ , and 13 min accumulation

**Table 2** Raman frequencies for type 2 sites in azurins

Azurin	Raman frequency and isotope shifts to lower energy ( $\text{cm}^{-1}$ )					
H117G(His-2)	259	296	319	350	388	424
$^{32}\text{S} \rightarrow ^{34}\text{S}$	-1.1	-0.7	-1.9			
$^{63}\text{Cu} \rightarrow ^{65}\text{Cu}$	-2.5	-0.8	-0.5			
$^{14}\text{N} \rightarrow ^{15}\text{N}$ -His	-0.9					
H117G(Aqua-2) <sup>a</sup>	268	296	321	357	387	426
$\text{H}_2\text{O} \rightarrow \text{D}_2\text{O}$	-1.3	-0.3	-0.5	-1.7	-0.8	-1.3
H46G(Im-2) <sup>b</sup>	261	295	325	337	353	388

<sup>a</sup> No isotope shifts detected with  $\text{H}_2^{18}\text{O}$

<sup>b</sup> No isotope shifts detected with  $^{15}\text{N}$ -imidazole

H117G(His-2) complex with  $^{65}\text{Cu}$  results in shifts at 259 ( $-2.5$ ), 296 ( $-0.8$ ) and 319 ( $-0.5$ )  $\text{cm}^{-1}$  (Fig. 5B) that are similar to the  $^{32}\text{S} \rightarrow ^{34}\text{S}$  shifts of  $-1.1$ ,  $-0.7$  and  $-1.9\text{ cm}^{-1}$  in these same three bands (Table 2). Thus, the majority of the Cu isotope dependence results from kinematic coupling of Cu–S(Cys) modes rather than Cu–N(His) modes.

Reconstitution of H46G-azurin with exogenous imidazole results in the formation of two different species, the H46G(Im-1) complex detected with 647-nm excita-

tion (Fig. 3C) and the H46G(Im-2) complex detected with 413-nm excitation (Fig. 5C). The RR spectrum of the H46G(Im-2) complex is similar to that of H117G(His-2) and H117G(Aqua-2), implying that it is a type 2 species with four strong ligands (proposed to be endogenous His and Cys, exogenous Im and  $\text{H}_2\text{O}$ ) in a square planar array. The  $^{15}\text{N}$ -imidazole complex of H46G(Im-2) exhibits no N isotope dependence whatsoever (Fig. 5C), again showing that imidazole ligands do not contribute significantly to the RR spectra of either type 1 or type 2 sites.

As in the case of the H46G-azurin complexes with imidazole, H117G-azurin can form both type 1 and type 2 complexes when it has only aqua ligands available at pH 6. The H117G(Aqua-1) and H117G(Aqua-2) complexes were investigated in  $\text{H}_2^{18}\text{O}$  in order to determine whether any of the RR spectral features were due to Cu–OH<sub>2</sub> vibrations. For inorganic complexes, terminal M–OH<sub>2</sub> vibrations occur between 300 and 500  $\text{cm}^{-1}$  [23–25] with predicted  $^{18}\text{O}$  isotope downshifts of 15–25  $\text{cm}^{-1}$ . However, no  $^{18}\text{O}$  effect is observed in the RR spectra of either the H117G(Aqua-1) or (Aqua-2) species (Fig. 6). Similarly,  $^{18}\text{O}$  exchange experiments on H46G(Aqua-1) and (Aqua-2) complexes also failed to

reveal any evidence of Cu–OH<sub>2</sub> vibrations (data not shown). In contrast, D<sub>2</sub>O exchange caused significant shifts of almost every RR mode in the spectra of the His117G(Aqua-1) and (Aqua-2) complexes (Tables 1,2), implying that the D-shifts of type 2 as well as type 1 sites are mainly due to cysteine amide NH vibrations. These observations lend further support to the view that the RR spectra of Cu-cysteinate proteins are dominated by modes from the Cu-Cys moiety, regardless of the presence of other ligands.

### Cysteine ligand fundamentals at higher energies

The RR spectra of both type 1 and type 2 azurins contain weak bands between 500 and 1500 cm<sup>-1</sup> (Fig. 7) that lie beyond the energies of Cu-ligand vibrations. In type 1 sites, these high frequency modes include combinations of the Cu–S stretch with other low frequency fundamentals [7], as well as several bands that are fundamentals in their own right. Thus, in wild-type azurin the  $\nu(\text{Cu–S})$  at 408 cm<sup>-1</sup> accounts for combination bands at 693, 780, 809, 836, and 1155, leaving the bands at 657, 753, 1226, and 1407 cm<sup>-1</sup> as fundamentals (Fig. 7A, Table 3). Similar high frequency fundamen-

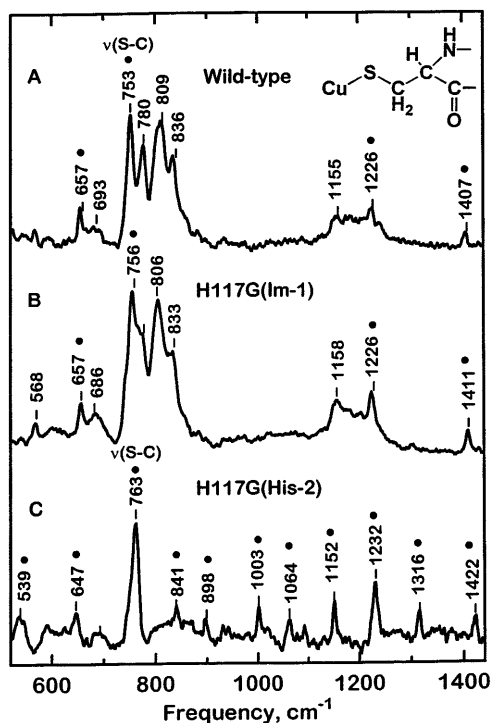


**Fig. 7A–C** High frequency Raman spectra of type 1 and type 2 sites. **A** Wild-type azurin, spectrum obtained as in Fig. 2 except for 7-cm<sup>-1</sup> resolution and 14 accumulations. **B** Imidazole adduct of H117G-azurin, spectrum obtained as in Fig. 2 except for 7-cm<sup>-1</sup> resolution. **C** Histidine adduct of H117G azurin, spectrum obtained as in Fig. 5. Peak frequencies marked with a *dot* denote fundamental modes of the Cu-cysteinate chromophore whose <sup>34</sup>S- and <sup>15</sup>N-shifts are listed in Table 3. Unmarked peaks are combination bands whose assignments are given in Table 3

tals are distinguished at 657, 756, 1226, and 1411 cm<sup>-1</sup> in the RR spectrum of the H117G(Im-1) complex (Fig. 7B). The combination band assignments are supported by the additivity of frequencies after <sup>15</sup>N and <sup>34</sup>S substitutions, as well as in the natural abundance samples (Table 3). Since these combination bands are completely missing from type 2 sites, all of the 11 high-frequency RR modes in the H117G(His-2) complex are assigned as fundamentals (Fig. 7C).

What are these high-frequency fundamentals? Since they are not observed upon Raman excitation of the apoprotein and their frequencies do not correspond to typical protein vibrational modes [26], they must be vibrations that are resonance-enhanced via the Cu-thiolate chromophore. Contributions from imidazole ligands are ruled out by the fact that no isotope shifts are observed in the high-frequency region for either H117G(Im-1) or H117G(His-2) prepared with <sup>15</sup>N labeling in the imidazole ring. Instead, there is a significant correlation with the vibrational modes of free cysteine, whose Raman spectrum has been completely assigned by normal coordinate analysis [27, 28]. In fact, ten of the high-frequency modes of H117G(His-2) appear to correspond to known vibrational modes of L-cysteine (Table 3). This is an impressive correlation considering that the cysteine in the H117G(His-2) site differs from free L-cysteine in the presence of amide linkages and Cu coordination. In addition its Raman intensities are constrained by the requirement that vibrational motions of the copper cysteinate must undergo alteration in the electronic excited state in order to show resonance enhancement. Other type 2 copper-cysteinate sites such as H117G(Aqua-2) complex do not exhibit such strongly enhanced cysteine ligand fundamentals.

The isotope dependence of the azurin RR spectra provides support for the cysteine assignments proposed in Table 3. Thus, global labeling of wild-type azurin with <sup>15</sup>N has its greatest effect on the 655-cm<sup>-1</sup> mode, which is calculated to have significant C<sub>α</sub>-N stretching character. After global labeling of H117G with <sup>34</sup>S, the most significant S isotope dependence occurs at 756 cm<sup>-1</sup> in the (Im-1) complex and at 763 cm<sup>-1</sup> in the (His-2) complex. This mode was assigned to  $\nu(\text{S–C}_\beta)$  on the basis of its S isotope shift and the observation that the *increased* S–C<sub>β</sub> bond strength in type 2 sites correlates with a *decrease* in Cu–S bond strength [7]. The 753-cm<sup>-1</sup> peak of wild-type azurin has also been designated as  $\nu(\text{S–C}_\beta)$  from its <sup>34</sup>S shift of –2 cm<sup>-1</sup> and a D shift of –51 cm<sup>-1</sup> upon substitution of the cysteine aliphatic hydrogens [20]. For both the H117G(His-2) complex and L-cysteine, the  $\nu(\text{S–C}_\beta)$  mode represents the most intense spectral feature in the 500–1500-cm<sup>-1</sup> region. The significantly higher energy of this vibration in the proteins compared to the 696-cm<sup>-1</sup> value for L-cysteine most likely reflects a difference in cysteine conformation:  $\nu(\text{S–C})$  frequencies in aliphatic thiols have been found to be highly sensitive to the S–C–C–C torsion angle [28]. The 1226-cm<sup>-1</sup> peak can be assigned



**Table 3** Raman frequencies of  $\nu(\text{Cu-S})$  combination bands and cysteine ligand fundamentals<sup>a</sup>

Wild-type		H117G(Im-1)		H117G(His-2)		L-cysteine <sup>b</sup>	Assignment <sup>c</sup>
$\nu$	$\Delta^{15\text{N}}$	$\nu$	$\Delta^{34\text{S}}$	$\nu$	$\Delta^{34\text{S}}$	$\nu$	
Combination bands							
693	-?	686	-3				408 + 284
780	-1	780	-?				408 + 372
809	-3	806	-?				408 + 400
836	-5	833	-4				408 + 428
1155	-?	1158	-4				408 + 753
Fundamentals							
657	-5	657	0	647	0	642	$\nu(\text{C}_{\alpha}\text{-N})$
753	0	756	-2	763	-3	696	$\nu(\text{S-C}_{\beta})$
				841	0	773	
				898	0	825	
						870	
						943	
				1003	0	1004	
				1064	0	1068	
				1152	0	1110	
1226	-1	1226	0	1232	0	1201	$\delta(\text{CNH})$
						1273	
				1316	0	1300	$\delta(\text{CCH})$
						1351	
						1400	
1407	-1	1411	0	1422	0	1427	$\delta(\text{HC}_{\beta}\text{H})$

<sup>a</sup> Frequencies ( $\nu$ ) and heavy isotope shifts to lower energy upon global labeling ( $\Delta$ ) in  $\text{cm}^{-1}$ . (-?) denotes shift of uncertain magnitude

<sup>b</sup> Raman spectrum of orthorhombic crystal of L-cysteine from [28]  
<sup>c</sup> Combination bands for wild-type azurin, fundamentals for L-cysteine from [28]

to the amide III mode of a peptide bond in a  $\beta$ -sheet-like conformation [26, 29]. Since this is primarily a C-N-H bend, it need not involve much movement of the central N atom. Finally the conserved vibration at  $\sim 1410 \text{ cm}^{-1}$  in type 1 azurins and at  $1422 \text{ cm}^{-1}$  in type 2 azurin appears to correspond to the  $1427\text{-cm}^{-1}$  mode in L-cysteine, which is assigned as a  $\text{CH}_2$  bend.

## Discussion

### Dominance of Cu-cysteinyl vibrations

Previous studies of copper-cysteinyl proteins have shown that the mode with the most substantial Cu-S stretching character is the one that exhibits the greatest Raman spectral intensity upon excitation within the (Cys)S $\rightarrow$ Cu CT band [7, 8, 18, 22]. The short Cu-S(Cys) bond of  $2.13 \text{ \AA}$  in wild-type azurin causes this mode to appear at  $408 \text{ cm}^{-1}$ , at much higher energy than the  $< 320 \text{ cm}^{-1}$  values for the  $2.25\text{- to }2.30\text{-\AA}$  Cu-S bonds of tetragonal Cu(II)-thiolate complexes and type 2 Cu-cysteinyl sites [7, 30]. In the present study, we have found that the influence of the cysteine ligand is not confined to the  $\nu(\text{Cu-S})$  region of the azurin RR spectrum, but instead extends from  $250$  to  $1500 \text{ cm}^{-1}$ . For type 1 sites,  $\nu(\text{Cu-S})$  character is partitioned among a cluster of vibrational modes at  $370\text{--}430 \text{ cm}^{-1}$  and their combination bands at  $780\text{--}1155 \text{ cm}^{-1}$ , all exhibiting substantial S-isotope dependence. The more extensive shifts upon global substitution with  $^{15}\text{N}$  (but not

upon substitution with  $^{15}\text{N}$ -imidazole) are ascribed to contributions from the amide N of the cysteine ligand and the amide Ns of neighboring peptide bonds. Thus, many of the remaining peaks in the  $250\text{--}1500 \text{ cm}^{-1}$  region can be assigned as cysteine fundamental vibrations. Further evidence for the predominant RR enhancement of cysteine ligand modes comes from the identification of the cysteine S-C $_{\beta}$  stretch at  $753 \text{ cm}^{-1}$  (Table 3) and the lack of any significant spectral contributions from histidine, methionine, or water ligands. Type 2 Cu-cysteinyl sites have their  $\nu(\text{Cu-S})$  cluster at lower energy, exhibit no combination bands, and can have a more extensive set of resonance-enhanced fundamentals that agree well with the known vibrational modes of the free amino acid, L-cysteine.

The involvement of His ligands in the RR spectrum of type 1 Cu proteins has long been debated. In a series of Cu-imidazole model complexes, the Raman active Cu-N(Im) symmetric stretch between  $245$  and  $288 \text{ cm}^{-1}$  was found to be too weakly resonance-enhanced to be detected in a protein unless it was associated with a stronger chromophore [31, 32]. Resonance-enhanced Cu-N(Im) stretching modes have been detected at  $265\text{--}365 \text{ cm}^{-1}$  in oxyhemocyanin because they are vibronically coupled to the peroxide  $\rightarrow$  Cu(II) CT transition [31, 33]. Similarly, in heme proteins, the axial Fe-N(His) bond stretches are in resonance with porphyrin electronic transitions and occur at  $\sim 220 \text{ cm}^{-1}$  in ferrous hemoglobin and myoglobin and at  $240\text{--}270 \text{ cm}^{-1}$  in peroxidases [34]. In contrast, oxyhemerythrin with five histidines ligated to an oxo-bridged diiron center has re-

vealed no Fe–N(His) vibrations at all [35]. In the present study of the H46G and H117G azurin mutants, replacement of either of the His ligands with an aqua ligand or substitution of  $^{15}\text{N}$ - for  $^{14}\text{N}$ -imidazole caused almost no change in the RR spectrum relative to that of wild-type azurin. The only noteworthy effects were shifts of  $-1\text{ cm}^{-1}$  in the  $286\text{-cm}^{-1}$  peak of the H117G(Im-1) complex (Fig. 4B) and the  $259\text{-cm}^{-1}$  peak of the H117G(His-2) complex (Fig. 5A). These results suggest that neither of the histidine ligands makes a significant contribution to the RR spectrum of azurin.

#### Enhancement by kinematic coupling with $\nu(\text{Cu-S})$

Cupredoxins exhibit a remarkably conserved set of RR frequencies despite coordination geometries ranging from trigonal to tetrahedral to square-planar [7, 13]. The constant background of frequencies has been ascribed to vibrations of the Cys ligand that remain relatively unaffected by changes at the copper site. What distinguishes these spectra is the location of the maximum RR intensity (associated with the Cu–S stretch) which occurs near  $400\text{ cm}^{-1}$  in type 1 sites and near  $300\text{ cm}^{-1}$  in type 2 sites, owing to their different Cu–S bond lengths of  $\sim 2.1$  and  $2.3\text{ \AA}$ , respectively. However, rather than being a single mode, Cu–S stretching character is distributed among several RR bands as shown by its S and Cu isotope dependence (Fig. 2A,B). The coupling is greatest with cysteine fundamentals that are closest in energy to the predominant Cu–S vibration, leading to a cluster of intense bands which are enhanced according to their share of the Cu–S stretching character. As the frequency of  $\nu(\text{Cu-S})$  varies among different cupredoxins, it couples more efficiently to Cys vibrations in different parts of the spectrum, leading to a different distribution of RR intensities, while keeping the pattern of frequencies essentially the same [7, 12, 13].

The Cu–S stretch is enhanced primarily by an A term mechanism [39] which is related to a displacement of atoms in the electronic excited state of the  $\text{S}\rightarrow\text{Cu}$  CT transition. However, the clustering of azurin Cu–S stretching character among several RR bands can be further ascribed to kinematic coupling of  $\nu(\text{Cu-S})$  with Cys ligand modes, a phenomenon of the electronic ground state whereby the Cu–S motion is physically joined with vibrations of neighboring atoms that are of similar energy. This type of vibrational mixing has also been observed in  $\text{Cu(II)}\{\text{HB}(3,5\text{-ipr}_2\text{pz})_3\}$  complexes with  $\text{SC}(\text{CH}_3)_3$  ligands that serve as models for thiolate binding in type 1 sites [36]. Although the most intense band at  $435\text{ cm}^{-1}$  was assigned as having the greatest  $\nu(\text{Cu-S})$  character by normal coordinate analysis, all of the RR modes were found to be sensitive to deuterium substitution or to changes in the structure of the thiolate ligand. Thus, it was concluded that all of the RR modes were mixed vibrations, that C–H motions were contributing to the mixing, and that the ability of kine-

matic coupling to extend over several atoms is highly dependent upon the conformation of the intervening atoms. In another study on  $\text{Fe}_2\text{S}_2(\text{Cys})_4$  ferredoxins, it was found that coplanarity of the atoms in the cysteine ligand greatly increases the tendency for kinematic coupling because Cys deformations such as the S–C–C bend lie in the same plane as the metal-sulfur stretch [37]. Azurin exhibits a similar arrangement whereby the five atoms of the  $\text{Cu-S}_\gamma\text{-C}_\beta\text{-C}_\alpha\text{-N}$  moiety are coplanar. This coplanarity appears to be highly conserved among cupredoxins [13] and is probably responsible for the extensive kinematic coupling of  $\nu(\text{Cu-S})$  with cysteine ligand modes in all of these proteins. The absence of such coupling in the RR spectra of Cu-cysteinate SOD mutants [30] and the  $\text{Cu}_A$  cluster of cytochrome *c* oxidase [38] may be due to the lack of a coplanar Cu-cysteinate.

#### Enhancement by extended Cu-Cys chromophore

It is clear that kinematic coupling of the Cu–S stretch with cysteine deformation modes does not explain all of the azurin RR vibrations. Whereas the S and Cu isotope dependencies track the most intense peaks of the spectrum in proportion to the fraction of Cu–S stretching character from kinematic coupling (Fig. 2A,B), the N and D isotope dependencies follow a totally different pattern (Fig. 2C,D). The fact that many of the N-sensitive bands show no measurable S isotope dependence suggests that their Raman enhancement does not involve physical coupling with the Cu–S stretch. Yet all of these vibrational modes exhibit RR excitation profiles that track the (Cys)S $\rightarrow$ Cu(II) CT band [40]. In these cases, it is likely that the enhancement is occurring mainly via the A term mechanism, which depends on a change in structure in the electronic excited state [39].

As noted above, the high RR intensity of the Cu–S stretch can be ascribed to an excited-state displacement along the Cu–S coordinate which results from excitation within a (Cys)S $\rightarrow$ Cu absorption band. If the chromophore extends beyond the Cu–S bond due to electronic delocalization, then other RR modes which are spatially and energetically remote from the Cu–S stretch can also be resonance enhanced, as long as the bonded atoms undergo a change in geometry during the S $\rightarrow$ Cu CT transition. In azurin, electrons in the  $\sigma$  framework of the cysteine side-chain may be delocalized into the  $\pi$  interaction between the  $\text{Cu}(dx_{2-y_2})$  and  $S(p)$  orbitals [41], thus extending the range of influence of the S $\rightarrow$ Cu CT transition. The N sensitivity of the azurin RR spectrum strongly supports the involvement of the cysteine amide. In addition, A term enhanced vibrations may extend even beyond the cysteine and into the polypeptide chain [42]. A recent normal coordinate analysis of azurin with data from isotopically labeled cysteine suggests that RR-active vibrations may include the polypeptide backbones of one or two residues on either side of the cysteine ligand [20].

## Conclusions

1. The Cu–S(Cys) stretch is the *only* metal-ligand vibration that undergoes significant resonance enhancement in the Raman spectrum of azurin. Histidine and H<sub>2</sub>O ligands (when present) generally do not contribute to the RR spectra of either type 1 or type 2 sites in mutant azurins, as evidenced by the lack of isotope shifts from <sup>15</sup>N-imidazole or <sup>18</sup>O-water.
2. The multiple RR modes of azurin originate predominantly from vibrations of the cysteine ligand, as indicated by their substantial isotope shifts upon global substitution with <sup>34</sup>S or <sup>15</sup>N. These peaks arise from at least two different mechanisms for resonance enhancement.
3. Cysteine vibrations that are close in energy and proximity to the Cu–S bond are resonance enhanced via ground-state kinematic coupling with the Cu–S stretch. This coupling is enhanced by the coplanarity of the Cu–S<sub>γ</sub>–C<sub>β</sub>–C<sub>α</sub>–N moiety. Such modes display S and Cu isotope shifts that are proportional to their  $\nu(\text{Cu-S})$  character.
4. Vibrations that are spatially or energetically remote from the Cu–S stretch are A term enhanced through an extended Cu–S(Cys) chromophore. In this case, the changes in geometry produced in the excited state of the S→Cu(II) CT transition are delocalized over several bond lengths, leading to extensive N isotope dependence.

**Acknowledgements** This work was supported by research grants from the National Institutes of Health (GM 18865 to J.S.-L. and T.M.L.) and the North Atlantic Treaty Organization (CRG 930170 and 951195 to T.M.L. and G.W.C.). We are grateful to Drs. Roman Czernuszewicz and Thomas G. Spiro for helpful discussions and for making their data available prior to publication.

## References

1. Sykes AG (1991) *Adv Inorg Chem* 36:377–408
2. Adman ET (1991) *Adv Protein Chem* 42:145–197
3. Baker EN (1988) *J Mol Biol* 203:1071–1095
4. Nar H, Messerschmidt A, Huber R, Kamp M van de, Canters GW (1991) *J Mol Biol* 221:765–772
5. Canters GW, Gilardi G (1993) *FEBS Lett* 325:39–48
6. Andrew CR, Sanders-Loehr J (1996) *Acc Chem Res* 29:365–372
7. Andrew CR, Yeom H, Valentine JS, Karlsson BG, Bonander N, Pouderoyen G van, Canters GW, Loehr TM, Sanders-Loehr J (1994) *J Am Chem Soc* 116:11489–11498
8. Dave BC, Germanas JP, Czernuszewicz RS (1993) *J Am Chem Soc* 115:12175–12176
9. Guss JM, Bartunik HD, Freeman HC (1992) *Acta Cryst B* 48:790–811
10. Pouderoyen G van, Andrew CR, Loehr TM, Sanders-Loehr J, Mazumdar S, Hill HAO, Canters GW (1996) *Biochemistry* 35:1397–1407
11. Blaauwen T den, Canters GW (1993) *J Am Chem Soc* 115:1121–1129
12. Blaauwen T den, Hoitink CWG, Canters GW, Han J, Loehr TM, Sanders-Loehr J (1993) *Biochemistry* 32:12455–12464
13. Han J, Adman ET, Beppu T, Codd R, Freeman HC, Huq L, Loehr TM, Sanders-Loehr J (1991) *Biochemistry* 30:10904–10913
14. Kamp M van de, Canters GW, Wijmenga SS, Lommen A, Hilbers CW, Nar H, Messerschmidt A, Huber R (1992) *Biochemistry* 31:10194–10207
15. Blaauwen T den, Kamp M van de, Canters GW (1991) *J Am Chem Soc* 113:5050–5052
16. Loehr TM, Sanders-Loehr J (1993) *Methods Enzymol* 226:431–470
17. Murphy LM, Strange RW, Karlsson BG, Lundberg L, Pascher T, Reinhammar B, Hasnain SS (1993) *Biochemistry* 32:1965–1975
18. Qiu D, Dong S, Ybe JA, Hecht MH, Spiro TG (1995) *J Am Chem Soc* 117:6443–6446
19. Nestor L, Larrabee JA, Woolery G, Reinhammar B, Spiro TG (1984) *Biochemistry* 23:1084–1093
20. Czernuszewicz RS, Fraczkiewicz G, Fraczkiewicz R, Dave BC, Germanas JP (1995) In: Merlin JC (ed) *Spectroscopy of biological molecules*. Kluwer, The Netherlands, pp 273–276
21. Mino Y, Loehr TM, Wada K, Matsubara H, Sanders-Loehr J (1987) *Biochemistry* 26:8059–8065
22. Blair DF, Campbell GW, Schoonover JR, Chan SI, Gray HB, Malmström BG, Pecht I, Swanson BI, Woodruff WH, Cho WK, English AM, Fry AF, Lum V, Norton KA (1985) *J Am Chem Soc* 107:5755–5766
23. Hester RE, Plane RA (1964) *Inorg Chem* 3:768
24. Adams DM, Lock PJ (1971) *J Chem Soc A*: 2801
25. Nakagawa I, Shimanouchi T (1964) *Spectrochim Acta* 20:429
26. Lord RC, Yu N-T (1970) *J Mol Biol* 50:509–524
27. Susi H, Byler M, Gerasimowicz WV (1983) *J Mol Struct* 102:63–79
28. Li H, Wurrey CJ, Thomas GJ Jr (1992) *J Am Chem Soc* 114:7463–7469
29. Frushour BG, Koenig JL (1975) In: Clark RJH, Hester RE (eds) *Advances in infrared and Raman spectroscopy*. Heyden, London, pp 35–97
30. Han J, Loehr TM, Lu Y, Valentine JS, Averill BA, Sanders-Loehr J (1993) *J Am Chem Soc* 115:4256–4263
31. Larrabee JA, Spiro TG (1980) *J Am Chem Soc* 102:4217–4223
32. Caswell DS, Spiro TG (1986) *J Am Chem Soc* 108:6470–6477
33. Ling J, Nestor LP, Czernuszewicz RS, Spiro TG, Fraczkiewicz R, Sharma KD, Loehr TM, Sanders-Loehr J (1994) *J Am Chem Soc* 116:7682–91
34. Teraoka J, Kitagawa T (1981) *J Biol Chem* 256:3936–3977
35. Sanders-Loehr J (1989) In: Loehr TM (ed) *Iron carriers and iron proteins*. VCH, New York, pp 373–466
36. Qiu D, Kilpatrick L, Kitajima N, Spiro TG (1994) *J Am Chem Soc* 116:2585–2590
37. Han S, Czernuszewicz RS, Spiro TG (1989) *J Am Chem Soc* 111:3496–3504
38. Andrew CR, Fraczkiewicz R, Czernuszewicz RS, Lappalainen P, Saraste M, Sanders-Loehr J (1996) *J Am Chem Soc* 118:10436–10445
39. Asher SA (1988) *Ann Rev Phys Chem* 39:537–588
40. Ainscough EW, Bingham AG, Brodie AM, Ellis WR, Gray HB, Loehr TM, Plowman JE, Norris GE, Baker EN (1987) *Biochemistry* 26:71–82
41. Solomon EI, Baldwin MJ, Lowery MD (1992) *Chem Rev* 92:521–542
42. Urushiyama A, Tobar J (1990) *Bull Chem Soc Jpn* 63:1563–1571